# Far-infrared electroluminescence characteristics of an InGaP/InGaAs/Ge triple-junction solar cell under forward DC bias*

Xiao Wenbo(肖文波)[1,†], He Xingdao(何兴道)[1], Gao Yiqing(高益庆)[1], Zhang Zhimin(张志敏)[1], and Liu Jiangtao(刘江涛)[2]

[1]Key Laboratory of Non-Destructive Test of Ministry of Education, Nanchang Hangkong University, Nanchang 330063, China
[2]Department of Physics, Nanchang University, Nanchang 330031, China

**Abstract:** The far-infrared electroluminescence characteristics of an InGaP/InGaAs/Ge solar cell are investigated under forward DC bias at room temperature in dark conditions. An electroluminescence viewgraph shows the clear device structures, and the electroluminescence intensity is shown to increases exponentially with bias voltage and linearly with bias current. The results can be interpreted using an equivalent circuit of a single ideal diode model for triple-junction solar cells. The good fit between the measured and calculated data proves the above conclusions. This work is of guiding significance for current solar cell testing and research.

**Key words:** triple-junction solar cell; electroluminescence; characteristics
**DOI:** 10.1088/1674-4926/33/6/064008 **EEACC:** 2520

## 1. Introduction

Multijunction solar cells consisting of InGaP, (In)GaAs and Ge have the potential to achieve high conversion efficiencies of more than 50%, and are promising candidates for space and terrestrial applications[1, 2]. As a result, efforts have been made to fabricate InGaP/InGaAs/Ge heterophotoelements[3, 4], and to investigate the photoelectric phenomena on them[5–7]. Recently, electroluminescence (EL) imaging has been regarded as a novel tool for fast spatially resolved solar cell characterization[8], and can also yield absolute mappings of serial resistance[9], diffusion length[10, 11]and subcell properties[12, 13]. However, the characterization of these devices is still challenging. In fact, due to the lack of a comprehensive physical model to describe the far-infrared EL intensity of multi-junction solar cells, experimental results still remain elusive.

In this work, the bias voltage and current dependence of the far-infrared EL intensity of a triple-junction solar cell have been evaluated in detail. It is observed that electroluminescence viewgraphs show clear device structures, and that the EL intensity increases exponentially with bias voltage and linearly with bias current. These results can be interpreted using an equivalent circuit of a single ideal diode model for multijunction solar cells. The good fit between the measured and calculated data proves the above conclusions, and is of great guiding significance for current solar cell testing and research.

## 2. Experimental sample and setup

An InGaP/InGaAs/Ge triple-junction solar cell manufactured by Yin Sheng Technology Co Ltd is evaluated in this study. A schematic illustration of a solar cell is shown in the inset of Fig. 1. The subcells (InGaP, InGaAs and Ge junctions) were grown on a p-type Ge substrate using metalorganic chemical vapor deposition. In this structure, the thicknesses of an InGaP top subcell, an InGaAs middle subcell, and a Ge bottom subcell were about 1 $\mu$m, 3 $\mu$m and 2 $\mu$m, respectively. Two tunnel junctions whose thickness was about 0.03 $\mu$m were implemented and placed between each pair of three subcells. The Ge substrate was about 140 $\mu$m, and the whole device thickness about 175 $\mu$m. The Ag core covered with Au on the top subcell was used as the top electrical contact, and another contact on the back of the sample was formed in the same way. The cell size was $10 \times 10$ mm$^2$.

The inset (top right) is a GaInP/GaInAs/Ge triple-junction

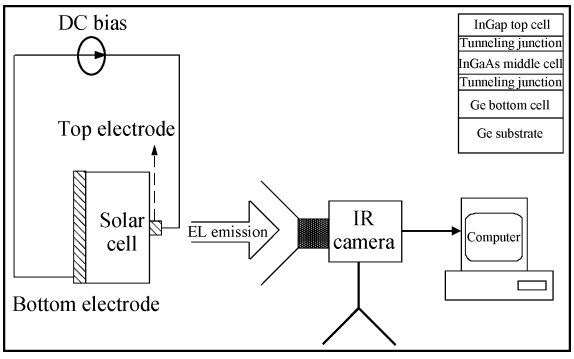


Fig. 1. Schematic diagram of the setup for electroluminescence measurement (not in scale).

* Project supported by the National Natural Science Foundation of China (Nos. 10904059, 41066001, 61072131, 61177096), the Aeronautical Science Foundation of China (No. 2010ZB56004), the Scientific Research Foundation of Jiangxi Provincial Department of Education (No. GJJ11176), the Open Fund of the Key Laboratory of Nondestructive Testing of Ministry of Education, Nanchang Hangkong University (No. ZD201029005), the Natural Science Foundation of Jiangxi Province, China (Nos. 2009GQW0017, 2009GZW0024), and the Graduate Innovation Base of Jiangxi Province, China.
† Corresponding author. Email: xiaowenbo1570@163.com
Received 16 November 2011, revised manuscript received 19 February 2012

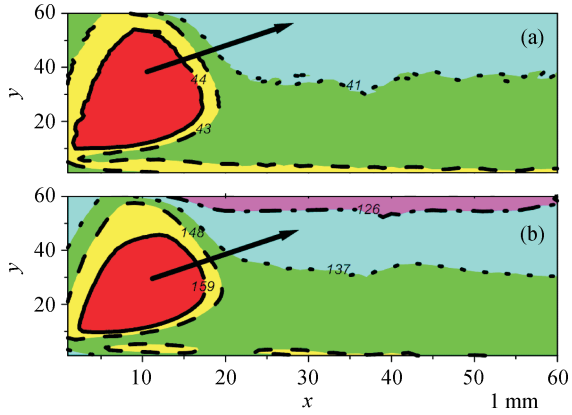


Fig. 2. (Color online) EL image map under forward DC bias voltages of (a) 2.8 V and (b) 3.0 V.

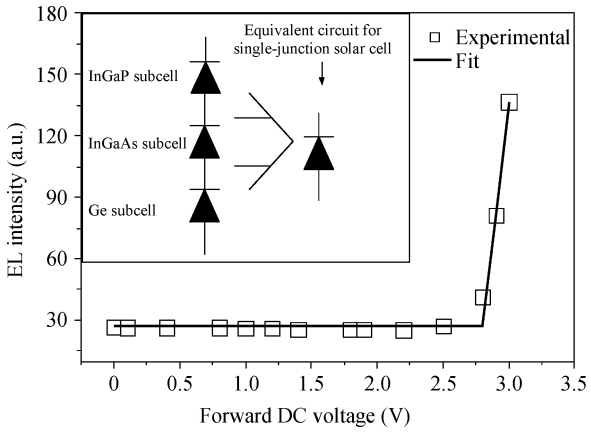


Fig. 3. EL intensity versus forward DC bias voltage. The inset (top left) is a schematic of the equivalent circuit model for the triple-junction solar cell, which can be simplified as a single large ideal diode.

solar cell structure.

Electroluminescence detection is performed by the setup as shown in Fig. 1. The sample is mounted in an $x$–$y$–$z$ micrometer positioner. When the solar cell works under certain forward bias conditions, the emitted photons can be captured with an infrared (IR) camera to obtain an image of the distribution of radiative recombination in the cell. In order to align the IR camera with the optical axis, the position of the solar cell can be adjusted by the positioner. Then the EL image is sent to a computer for calculation of the corresponding mean EL intensity. In this way, the EL intensity dependences of forward DC bias voltage and current are measured.

In the real experiment, the LM1719A power supply model is selected as a DC bias source. The camera (number VC hr Research 780 made by InfraTec GmbH) is used for data acquisition at a suitable resolution of 640 × 480 pixels, which has a linear response function. The camera works in a wavelength range from 7.5 to 14 $\mu$m. All the experiments are accomplished under room temperature and in dark conditions.

## 3. Results and discussion

In Fig. 2, a measured far-IR thermal image map is shown under a forward DC bias voltage of 2.8 V and 3.0 V. The contour curves in Fig. 2(a) correspond to the EL intensities of 44 (solid), 43 (dash), and 41 (dot), respectively. The red, yellow, green and cyan regions represent that the fluorescence intensity is > 44, > 43, > 41 and < 41. The contour curves in Fig. 2(b) correspond to the EL intensities of 159 (solid), 148 (dash), 137 (dot) and 126 (dash dot), respectively. The red, yellow, green, cyan and magenta regions represent that the fluorescence intensity is >159, >148, >137, >126 and <126. It can be seen that maximal light intensity exists in the vicinity of the top electrode. With the increase in distance from the electrode, the light intensity starts a gradual decline (indicated by the arrows in Fig. 2). This phenomenon can be interpreted as follows: for high carrier densities near the electrode region, there is a high recombination probability which leads to strong light intensity. Due to the effect of lateral diffusion, the magnitude of the current density will fall with distance from the electrode. Therefore, the luminescence intensity also decreases. It should be noted that there is no obvious difference in the EL images between the two bias conditions, and that no significant flaw is observed in this triple-junction solar cell from the EL images. After the bias voltage level is changed, the same results are also obtained.

In Fig. 3, the measured EL intensity as a function of the forward DC voltage is shown. It can be seen that there is not a simple linear relationship. It is noted that the intensity is nearly constant until approximately 2.7 V, and after that the curve is lifted up rapidly. In order to study the injection current effect on EL intensity, the EL intensity is measured against the forward DC current, as shown in Fig. 4. It is observed that the intensity is an almost linear increase with bias current.

Traditionally, it is widely regarded that the equivalent circuit model of triple-junction solar cells is composed of three diodes connected in series[5, 7]. In essence, the whole cell can be described as a single large ideal diode, as shown in the inset of Fig. 3. Therefore, a simple ideal diode model is used in this study. The total excess minority carrier number $N$ along the depth $x$ in the P active layer will be expressed as follows[11, 14]:

$$N = \int_0^{+\infty} n_{\rm p}(0)\exp(-x/L_{\rm e})\mathrm{d}x = n_{\rm p}(0)L_{\rm e}, \qquad (1)$$

in which $n_{\rm p}(0)$ is the excess minority carrier number at the p–n junction edge, and $L_{\rm e}$ is the diffusion length, which tends to a constant at room temperature .

$n_{\rm p}(0)$ is subject to an applied forward voltage $V$ by the following equation[15]:

$$n_{\rm p}(0) = n_{\rm p}\exp(eV/kT), \qquad (2)$$

where $n_{\rm p}$, $e$, $k$, and $T$ are the equilibrium minority carrier density in the P layer, the electron charge, the Boltzmann constant, and the temperature, respectively.

The EL intensity $I_{\rm EL}$ is considered to be proportional to $N$ integrated along the depth. Therefore, $I_{\rm EL}$ is also proportional to $n_{\rm p}(0)$ for fixed diffusion length $L_{\rm e}$. Then, $I_{\rm EL}$ will be expressed as a function of $V$ as follows:

$$I_{\rm EL} = A\exp(eV/kT), \qquad (3)$$

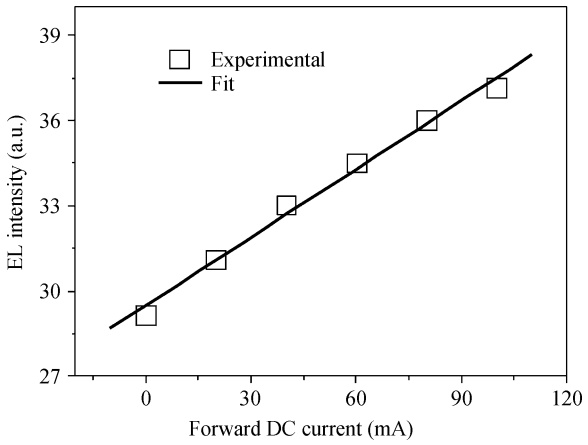


Fig. 4. EL intensity versus forward DC bias current.

where $A$ is a constant that is related to doping density and temperature.

Therefore, it is clear that EL intensity increases exponentially with bias voltage, which is behavior similar to a forward-biased ideal diode. After considering the background signal, a fitting curve is plotted in Fig. 3 according to Eq. (3). From the fitting results, good agreement can be observed. The extracted constant is about $(8.2394 \pm 1.2348) \times 10^{-49}$. Because the fitting errors do not exceed 15%, this model can provide a reasonable explanation of the experimental data.

In addition, the forward current $I$ of an ideal diode can be determined by the well-known Shockley diode equation, and an ideality factor of 1 is expected. Therefore,

$$I = I_0[\exp(eV/kT) - 1], \tag{4}$$

where $I_0$ is the dark reverse saturation current.

If condition $(\exp(eV/kT) \gg 1)$ is satisfied (which is true particularly when the bias voltage is large enough), then the above equation can be simplified as follows:

$$I \approx I_0 \exp(eV/kT). \tag{5}$$

Then, combing Eq. (3) and Eq. (5), the EL intensity follows that

$$I_{\mathrm{EL}} \approx A\frac{I}{I_0}, \quad I_{\mathrm{EL}} \propto I. \tag{6}$$

From Eq. (6), it is quite obvious that EL intensity is a linear function of the forward injection dc current. The corresponding fitting curve is shown in Fig. 4. The extracted slope is about $80.14299 \pm 3.87143$. The fitting errors do not exceed 4%, and the results are very close to the predicted relation. It should be noted that Equation (6) is completely different from the results for a single-junction solar cell given by Fuyuki *et al.*[16] and Mártil *et al.*[17], in which the diode ideality factor can be deduced by measuring the electroluminescence intensity as a function of the forward injection current. There may be two reasons for this. One is that the performances of the series-connected diodes depend on the characteristics of each diode, so the cell will be close to the ideal diode characteristics if all the diodes are perfect. Another is that the two tunnel junctions in the sample may reduce leakage current, so that the total cell current would be a diffusion current and the whole cell ideality factor would be 1. From the above results, it can be seen that there are no defects in this triple-junction solar cell. This conclusion is consistent with the findings from the far-infrared thermal image map in Fig. 2. The triple junction solar cell can therefore be regarded as a single large ideal diode in certain conditions.

## 4. Conclusion

The far-infrared electroluminescence characteristics of an InGaP/InGaAs/Ge triple-junction solar cell under forward dc bias were analyzed in detail. It is clearly observed that the electroluminescence viewgraph shows clear device structures, and that the EL intensity increases exponentially with bias voltage and linearly with bias current. These results can be interpreted using the equivalent circuit of a single ideal diode model for multijunction solar cells. The fitting results prove our proposed model. This work is very significant for the research, testing and production of solar cells.

## Acknowledgement

The authors would like to thank Lai X L, Wei Q and Ye J H for their support and help in the experimental process.

## References

[1] Yamaguchi M, Takamoto T, Araki K, et al. Multi-junction III–V solar cells: current status and future potential. Solar Energy, 2005, 79: 78

[2] Baur C, Bett A W, Dimroth F, et al. Triple-junction III–V based concentrator solar cells: perspectives and challenges. J Sol Energy Eng, 2007, 129: 258

[3] King R R, Law D C, Edmondson K M, et al. 40% efficient metamorphic GaInP/GaInAs/Ge multijunction solar cells. Appl Phys Lett, 2007, 90: 183516

[4] Guter W, Schöne J, Philipps S P, et al. Current-matched triple-junction solar cell reaching 41.1% conversion efficiency under concentrated sunlight. Appl Phys Lett, 2009, 94: 223504

[5] Nishioka K, Takamotob T, Agui T, et al. Evaluation of InGaP/InGaAs/Ge triple-junction solar cell and optimization of solar cell's structure focusing on series resistance for high-efficiency concentrator photovoltaic systems. Sol Energy Mater Sol Cells, 2006, 90: 1308

[6] Sato S, Miyamoto H, Imaizumi M, et al. Degradation modeling of InGaP/GaAs/Ge triple-junction solar cells irradiated with various-energy protons. Sol Energy Mater Sol Cells, 2009, 93: 768

[7] Nishioka K, Sueto T, Uchida M, et al. Detailed analysis of temperature characteristics of an InGaP/InGaAs/Ge triple-junction solar cell. J Electron Mater, 2010, 39: 704

[8] Breitenstein O, Bauer J, Trupke T, et al. On the detection of shunts in silicon solar cells by photo- and electroluminescence imaging. Prog Photovolt: Res Appl, 2008, 16: 325

[9] Hinken D, Ramspeck K, Bothe K, et al. Series resistance imaging of solar cells by voltage dependent electroluminescence. Appl Phys Lett, 2007, 91: 182104

[10] Fuyuki T, Kondo H, Yamazaki T, et al. Photographic surveying of minority carrier diffusion length in polycrystalline silicon solar cells by electroluminescence. Appl Phys Lett, 2005, 86: 262108

[11] Würfel P, Trupke T, Puzzer T, et al. Diffusion lengths of silicon solar cells from luminescence images. J Appl Phys, 2007, 101: 123110

[12] Kirchartz T, Rau U, Hermle M, et al. Internal voltages in GaInP/GaInAs/Ge multijunction solar cells determined by electroluminescence measurements. Appl Phys Lett, 2008, 92: 123502

[13] Zimmermann C G. Performance mapping of multijunction solar cells based on electroluminescence. IEEE Electron Device Lett, 2009, 30: 825

[14] Nelson J. The physics of solar cells. London: Imperial College Press, 2003: 145

[15] Sze S M, Ng K K. Physics of semiconductor devices. 3rd ed. Hoboken: John Wiley & Sons, 2007: 16

[16] Fuyuki T, Kondo H, Kaji Y, et al. Analytic findings in the electroluminescence characterization of crystalline silicon solar cells. J Appl Phys, 2007, 101: 023711

[17] Mártil I, Redondo E, Ojeda A. Influence of defects on the electrical and optical characteristics of blue light-emitting diodes based on III–V nitrides. J Appl Phys, 1997, 81: 2442